HEFAT2012
9th International Conference on Heat Transfer, Fluid Mechanics and Thermodynamics
16 – 18 July 2012
Malta

DEFORMATION OF LIQUID DROPS CONTAINING IONS IN THE PRESENCE OF AN ELECTRIC FIELD

Berry J. D., Davidson M.R.* and Harvie D.J.E.
*Author for correspondence
Department of Chemical and Biomolecular Engineering,
University of Melbourne,
Victoria, 3010,
Australia,
E-mail: m.davidson@unimelb.edu.au

ABSTRACT

The deformation and breakup of a conducting water drop immersed in hexadecane in the presence of an electric field is investigated using a numerical tool for a range of field strengths and ion concentrations. At low electric field strengths, the drop deformation is a linear function of the electric capillary number. For high electric field strengths, the dependence is no longer linear, and significant drop deformation occurs. The drop deformation increases with increasing ion concentration, due to a separation of ions within the drop, leading to a redistribution of charge at either end of the drop.

INTRODUCTION

Detailed understanding of the physics of drops in the presence of an electric field is vital for developing more efficient technologies for applications such as ink-jet printing, drug delivery, and sample analysis [1-4]. In particular, the field of microfluidics requires precise control over the formation, motion, coalescence and breakup of drops [5-7]. An efficient method of controlling these phenomena is to exploit the electrical properties of the fluids in question with the application of an external electric field. When one or more liquids present in the device is an electrolyte, the presence of ions in the flow further complicates the physics involved [8].

There are numerous theoretical descriptions of small drop deformation in the presence of a small external electric field. The field of electrohydrostatics considers two distinct limits: a perfect dielectric drop immersed in a perfect dielectric medium, with no free charges present, or a highly conducting drop immersed in a perfect dielectric medium, again with no free charges present [9]. In both cases, the electrical stress acts normal to the interface, and can therefore be balanced by interfacial tension. In such cases the drop can only deform prolately (in the direction of the electric field). Because the electric force only acts normal to the interface, there is no tangential electric stress present at equilibrium to drive fluid flow.

In the leaky dielectric model, drops of small but finite conductivity are considered, giving rise to an accumulation of electrical charge at the interface [10]. The presence of interfacial charge permits tangential electrical stresses, leading to fluid flow at equilibrium. The drop is able to deform both prolately and oblately. The deformation of electrolytic drops in an electrolytic medium has also been considered, with free charges present in the fluid bulk [11]. This analytical study provides the basis for comparison to the numerical results presented in this paper.

These types of analyses are restricted to small drop deformation and low electric-field strength. This study uses a numerical model to characterise the deformation of a drop for arbitrary field strengths and ion concentrations within the drop. In particular a water drop containing free ions, suspended in non-conducting hexadecane, will be analysed. This case is typical of common water-in-oil systems [12,13].

NOMENCLATURE

a	Drop axis normal to electric field
b	Drop axis parallel to electric field
Ca_V	Capillary number (ratio of viscous to interfacial tension forces)
Ca_E	Electric capillary number (ratio of electric to interfacial tension forces)
D	Taylor deformation parameter (Eq. 7)
e	Elementary charge
$\boldsymbol{E}$	Electric field vector
E_{ref}	Electric field scale
$\boldsymbol{f_E}$	Electric body force
$\boldsymbol{f_s}$	Interfacial tension force
h	Computational cell width
$\boldsymbol{I}$	Identity matrix
k	Boltzmann constant
K	Dimensionless inverse Debye length
M	Viscosity ratio μ_d/μ_c
n_+	Positive ion concentration
n_-	Negative ion concentration

n_0	Reference ion concentration
P	Pressure
Pe	Peclet number
R	Initial drop radius
Re	Reynolds number
S	Permittivity ratio $\varepsilon_d/\varepsilon_c$
t	Time
T	Temperature
$\boldsymbol{u}$	Velocity vector
V	Velocity scale
We	Weber number
z	Ion valence

Special characters

α	Ion diffusivity
γ	Surface tension
δ_s	Dirac delta function at fluid interface
ε	Fluid permittivity
ε_0	Permittivity of free space
μ	Fluid viscosity
ρ	Fluid density
ϕ	Disperse-phase volume fraction

Subscripts

c	Continuous phase
d	Disperse phase
0	Ambient or reference

NUMERICAL METHOD

The equations governing the fluid flow, the electric field, and the ion transport are non-dimensionalised with velocity scale V, length scale R, time scale R/V, ion number density scale n_0, and electric field scale $E_{ref} = kT/zeR$. The dimensionless equations are

$$\frac{\partial \phi}{\partial t} + \nabla \cdot \phi \boldsymbol{u} = 0, \tag{1}$$

$$\nabla \cdot \boldsymbol{u} = 0, \tag{2}$$

$$\frac{\partial \rho \boldsymbol{u}}{\partial t} + \nabla \cdot (\rho \boldsymbol{u}\boldsymbol{u}) = -\nabla P + \frac{1}{\mathrm{Re}} \nabla \cdot \mu \left[\nabla \boldsymbol{u} + (\nabla \boldsymbol{u})^T \right] + \frac{1}{\mathrm{We}} \delta_s \boldsymbol{f}_s + \frac{\mathrm{Ca_E}}{\mathrm{We}} \boldsymbol{f}_E, \tag{3}$$

$$\nabla \cdot \varepsilon \boldsymbol{E} = \frac{1}{2} K^2 S \left(n_+ - n_- \right), \tag{4}$$

$$\frac{\partial \phi n_\pm}{\partial t} + \nabla \cdot (\boldsymbol{u} \phi n_\pm) = \frac{1}{\mathrm{Pe}} \nabla \cdot \left[\phi \nabla n_\pm \mp \phi n_\pm \boldsymbol{E} \right], \tag{5}$$

where (1) is the disperse-phase volume fraction transport equation; (2) is the continuity equation; (3) is the momentum equation; (4) is the Poisson equation for the electric field; and (5) is the ion transport equation for both anions and cations, formulated to give zero ion flux at the interface. The dimensionless groups governing the flow are

$$\mathrm{Re} = \frac{\rho_c V R}{\mu_c}, \; We = \frac{\rho_c V^2 R}{\gamma}, \; \mathrm{Ca_E} = \frac{\varepsilon_0 \varepsilon_c {E_{ref}}^2 R}{\gamma}, \quad \mathrm{K} = \left[\frac{2 z^2 e^2 n_0 R^2}{\varepsilon_0 \varepsilon_d k T} \right]^{\frac{1}{2}}, \text{ and } \mathrm{Pe} = \frac{VR}{\alpha}. \tag{6}$$

Here, the electric capillary number $\mathrm{Ca_E}$ represents the relative importance of electric forces to interfacial tension forces. This is analogous to the viscous capillary number $\mathrm{Ca_V} = \mu_C V/R$, which measures the relative importance of viscous forces to interfacial tension forces. The velocity scale V is chosen such that the Reynolds number Re=0.1. The dimensionless density ρ, viscosity μ, and permittivity ε are scaled by the continuous phase values. At interface cells, these quantities are calculated using averaging weighted by the volume fraction value in the interface cell [15-17]. The dimensionless inverse Debye length K is scaled using the discrete fluid permittivity ε_d.

The transient, multiphase finite volume method of Rudman [14] has been adapted to include electrokinetic effects. The single-phase implementation is given in Davidson and Harvie [15], and the combined level-set, volume of fluid adaptation is given in Harvie et al. [16]. Details of the ion transport algorithm for multiphase electrokinetic flows are given in Berry et al. [17].

Calculations are performed on a uniform grid with cell-spacing h/R = 1/16. When the dimensionless inverse Debye length K is finite, the water drop contains cations and anions of equal diffusivities $\alpha_+ = \alpha_- = \alpha$ and equal valencies $z_+ = -z_- = z$. Initially, the drop is spherical, and the dimensionless ion concentrations in the drop are set to $n_+ = n_- = 1$, and zero outside. The Reynolds number and Weber number are set to Re=0.1 and We=0.1 (giving a capillary number $Ca_V = 1$). The Peclet number is Pe = 1. A uniform electric field E =1 is then imposed on the domain (Fig. 1).

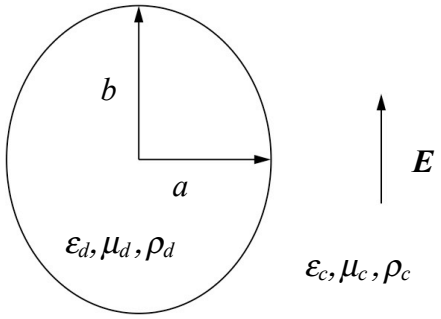

Figure 1 Schematic of water drop immersed in hexadecane.

The uniform electric field acts to deform the drop, until steady-state is reached, or drop breakup occurs. The steady-state drop deformation is quantified using the Taylor deformation parameter D, defined as

$$D = \frac{b-a}{b+a} \tag{7}$$

Increasing the mesh-resolution by a factor of two yields a difference in Taylor deformation parameter of less than 3%. For numerical convenience, the governing equations are solved in terms of an electric potential U, instead of the electric-field vector $\boldsymbol{E}$. The electric potential is defined by

$$\boldsymbol{E} = -\nabla U. \tag{8}$$

RESULTS AND DISCUSSION

Results are presented here for a water drop immersed in hexadecane with viscosity ratio M = 0.1 and permittivity ratio S = 40. The electric capillary number (representing field strength) range investigated is $0.01 \leq Ca_E \leq 0.25$. The dimensionless inverse Debye length K, representing ion concentration in the drop, is varied between 0 and 5, giving diffuse regions of charge in the drop at steady state.

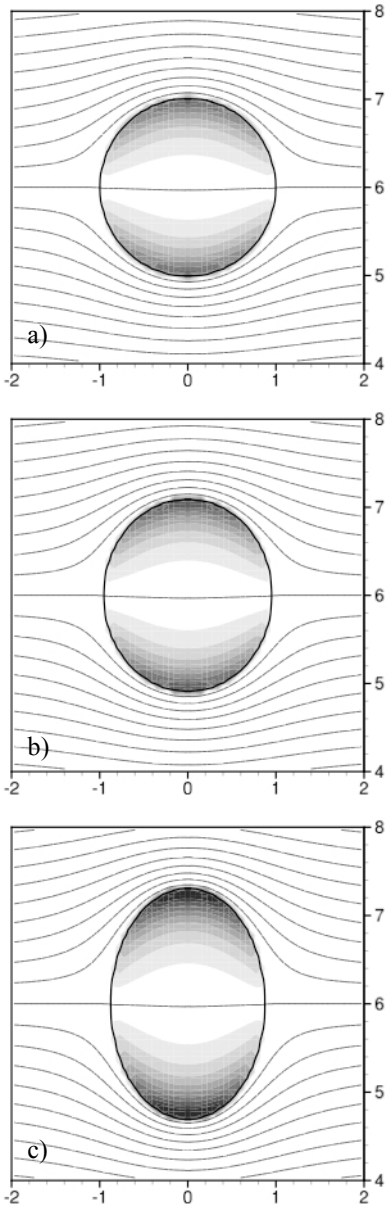

Figure 2 Contours of charge density magnitude $|n_+\text{-}n_-|$ within the steady-state drop and electric potential for dimensionless inverse Debye lengh K = 4, and electric capillary number a) $Ca_E = 0.01$ ($|n_+\text{-}n_-|_{MAX.} = 0.037$), b) $Ca_E = 0.10$ ($|n_+\text{-}n_-|_{MAX.} = 0.039$), and c) $Ca_E = 0.20$ ($|n_+\text{-}n_-|_{MAX.} = 0.051$). The electric potential contour line spacing is 0.2.

Fig. 2 shows the steady-state deformation of the drop for dimensionless inverse Debye length K = 4, and three increasing electric capillary numbers. Also depicted are the contours of charge-density magnitude (defined as $|n_+\text{-}n_-|$), and contours of electric potential U. Because the permittivity ratio S is large, the electric field magnitude inside the drop is much smaller than the electric field magnitude outside the drop. As a consequence the electric potential contours are not shown inside the drop.

As the field strength increases, the drop elongates in the direction of the field. This behaviour is consistent with the behaviour of drops without ions: the electric force acting on the bound polarized electric charges at the interface, due to the permittivity difference between the two phases, deforms the drop until the interfacial tension force is able to arrest the deformation.

The electric force in that case is given by

$$\boldsymbol{f}_E = -\frac{1}{2}\boldsymbol{E}\cdot\boldsymbol{E}\,\nabla\varepsilon. \tag{9}$$

The drop deforms because the electric-field magnitude varies along the interface. However the electric force only acts normal to the interface, and as a consequence no flow is present at equilibrium when no ions are present.

When ions are present in the drop, as is the case in Fig.2, there is an extra electric force component and the total electric force is given by

$$\boldsymbol{f}_E = -\frac{1}{2}\boldsymbol{E}\cdot\boldsymbol{E}\,\nabla\varepsilon + \frac{1}{2}K^2 S(n_+ - n_-)\boldsymbol{E}. \tag{10}$$

Regions of net charge $n_+\text{-}n_-$ are able to form, and the electric field acts on both the induced charge and the bound polarized charges at the interface. The electric force due to induced charge is in the direction of the local electric field, and is therefore not in general normal to the interface. Hence, tangential electric stress may be present at equilibrium, leading to steady-state fluid flow.

The presence of the electric field causes the cations inside the drop to move to one side of the drop, and the anions to the other (Fig. 2). A consequence of the charge separation is a buildup of charge at either end of the elongated drop. The electric field acts on this induced charge to deform the drop further. As the electric field strength increases, the ions become more concentrated at either end of the drop, leading to larger charge accumulation and hence larger deformation.

Interestingly the contours of electric potential run parallel to the drop interface, meaning that the direction of the electric field, and hence the electric force, is normal to the interface. Thus there is no steady-state flow for this particular system. For the cases shown in Fig. 2, the maximum velocity magnitude is $O(10^{-2})$, indicating that no flow is present.

When the electric capillary number is large enough, the drop deformation accelerates with time and drop breakup occurs. Fig. 3 shows a drop with dimensionless inverse Debye length K = 4 and electric capillary number $Ca_E = 0.25$ at time t = 15. The electric field and the charge density magnitude at the drop tip is extremely large relative to the steady-state values

shown in Fig. 3. The electric force will continue to elongate the drop in the direction of the electric field until fragmentation occurs.

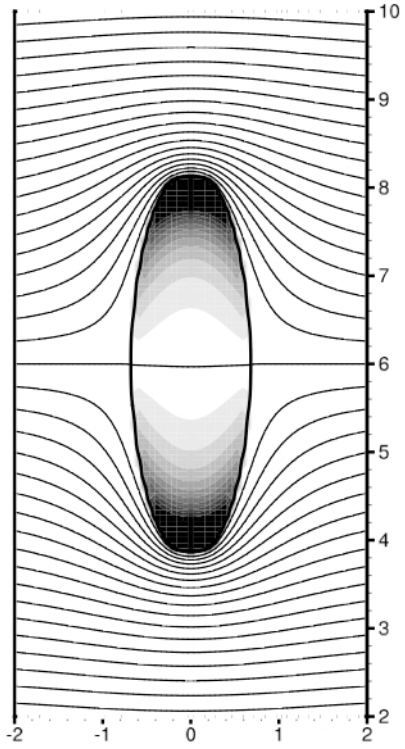

Figure 3 Contours of charge density magnitude $|n_+\text{-}n_-|$ within the drop and electric potential for dimensionless inverse Debye lengh K = 4, and electric capillary number $Ca_E = 0.25$ at time t=15 ($|n_+\text{-}n_-|_{MAX.} = 0.12$). The electric potential contour line spacing is 0.2.

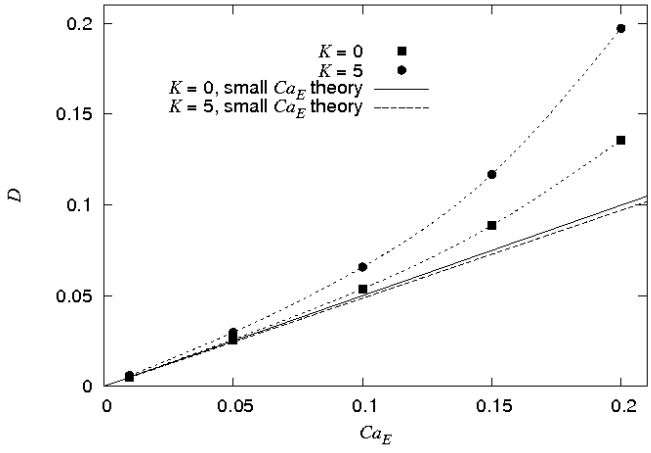

Figure 4 Variation of deformation parameter D with electric capillary number Ca_E.

The analysis of Zholkovskij et al. [11] demonstrated that for low field strengths, the drop deformation is linearly proportional to the electric capillary number. The analytical solution is plotted in Fig. 4, along with the numerical results for dimensionless inverse Debye lengths K = 0, and K = 5.

At low values of electric capillary number, the numerical results show good agreement with the analytical solution. As the electric capillary number becomes significant, the dependence of the drop deformation parameter on the electric capillary number is no longer linear. For significant values of electric capillary number, the drop deformation is much higher than predicted from the theory. When there are no ions present in the drop (the K = 0 case), the drop deformation is less than that for the case where ions are present (K = 5). The highest deformation resulting from the simulation is ~100% larger than the analytical prediction, formulated for small Ca_E. The increased deformation for the finite K case is due to the buildup of charge at each end of the drop, thereby increasing the electrical force acting to deform the drop along the direction of the electric field.

The full parameter space investigated is shown in Fig. 5. Here, the Taylor deformation parameter has been normalized by the electric capillary number and plotted as a function of dimensionless inverse Debye length. For small values of electric capillary number, the normalized drop deformation parameter D/Ca_E becomes independent of Ca_E and approaches the analytical solution of Zholkovskij et al. [11]. The deformation of the drop increases with increasing dimensionless inverse Debye length K, due to the accumulation of charge inside the drop. This effect becomes more pronounced as the electric capillary number increases.

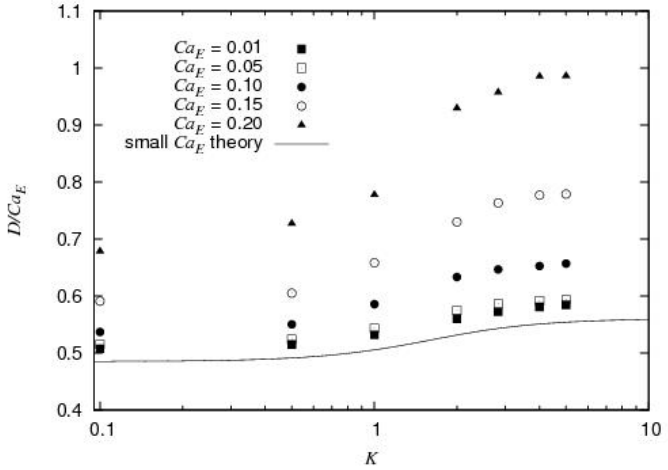

Figure 5 Variation of normalised deformation parameter D/Ca_E with dimensionless inverse Debye length, K.

CONCLUSIONS

The deformation and breakup of a water drop containing ions immersed in hexadecane in the presence of an electric field has been studied with a computational fluid dynamics algorithm for a range of electric-field strengths and ion concentrations.

For low electric-field strengths, the drop deformation is a linear function of the electric capillary number Ca_E, consistent with the theory of Zholkovskij et al. [11]. For high field

strengths, the dependence is no longer linear, and significant drop deformation occurs over and above the small field strength theory. When ions are present in the drop, separation of anions and cations occurs at either end of the drop. The subsequent charge accumulation causes the drop to deform significantly more than if no ions are present, due to the extra electrical force present acting on the accumulated charge.

ACKNOWLEDGEMENTS

This research was supported by the Australian Research Council Grants Scheme and by computational resources on the National Computational Infrastructure Facility through the National Computational Merit Allocation Scheme.

REFERENCES

[1] J. Eggers, Nonlinear dynamics and breakup of free-surface flows, *Review of Modern Physics,* Vol. 69 (3), 1997, pp. 865–929

[2] J.-U. Park, M. Hardy, S. J. Kang, K. Barton, K. Adair, D. K. Mukhopadhyay, C. Y. Lee, M. S. Strano, A. G. Alleyne, J. G. Georgiadis, P. M. Ferreira, J. A. Rogers, High-resolution electrohydrodynamic jet printing, *Nature Materials*, Vol. 6 (10), 2007, pp. 782–9

[3] F. Li, O. Ozen, N. Aubry, D. T. Papageorgiou, P. G. Petropoulos, Linear stability of a two-fluid interface for electrohydrodynamic mixing in a channel, *Journal of Fluid Mechanics*, Vol. 583, 2007, pp. 347

[4] J. D. Zahn, V. Reddy, Two phase micromixing and analysis using electrohydrodynamic instabilities, *Microfluidics and Nanofluidics*, Vol. 2 (5), 2006, pp. 399–415

[5] K. Ahn, C. Kerbage, T. P. Hunt, R. M. Westervelt, D. R. Link, D. A. Weitz, Dielectrophoretic manipulation of drops for high-speed microfluidic sorting devices, *Applied Physics Letters*, Vol. 88 (2), 2006, 024104

[6] K. Ahn, J. Agresti, H. Chong,M.Marquez, D. a.Weitz, Electrocoalescence of drops synchronized by size-dependent flow in microfluidic channels, *Applied Physics Letters*, Vol. 88 (26), 2006, 264105

[7] H. Gu, C. U. Murade, M. H. G. Duits, F. Mugele, A microfluidic platform for on-demand formation and merging of microdroplets using electric control, *Biomicrofluidics*, Vol. 5 (1), 2011, 11101

[8] N. A. Mishchuk, Concentration polarization of interface and non-linear electrokinetic phenomena, *Advances in Colloid and Interface Science*, Vol. 160, 2010, pp. 16–39

[9] J. R. Melcher, G. I. Taylor, Electrohydrodynamics: A review of the role of interfacial shear stresses, *Annual Review of Fluid Mechanics*, Vol. 1 (1), 1969, pp. 111–146

[10] G.I. Taylor, Studies in electrohydrodynamics. I. The circulation produced in a drop by electrical field, *Proceedings of the Royal Society A: Mathematical, Physical and Engineering Sciences*, Vol. 291 (1425), 1966, pp. 159–166

[11] E. K. Zholkovskij, J. H. Masliyah, J. Czarnecki, An electrokinetic model of drop deformation in an electric field, *Journal of Fluid Mechanics*, Vol. 472, 2002, pp. 1–27

[12] J. Xu, D. Attinger, Drop on demand in a microfluidic chip, *Journal of Micromechanics and Microengineering*, Vol. 18 (6), 2008, 065020

[13] K. Ahn, C. Kerbage, T. P. Hunt, R. M. Westervelt, D. R. Link, D. A. Weitz, Dielectrophoretic manipulation of drops for high-speed microfluidic sorting devices, *Applied Physics Letters*, Vol. 88 (2), 2006, 024104

[14] M. Rudman, A volume-tracking method for incompressible multifluid flows with large density variations*, International Journal for Numerical Methods in Fluids*, Vol. 28, 1998, pp. 357–378

[15] M. Davidson, D. Harvie, Electroviscous effects in low Reynolds number liquid flow through a slit-like microfluidic contraction, *Chemical Engineering Science*, Vol. 62 (16), 2007, pp. 4229–4240

[16] D. J. E. Harvie, M. Rudman, M. R. Davidson, Parasitic current generation in Combined Level Set and Volume of Fluid immiscible fluid simulations, *ANZIAM Journal*, Vol. 48, 2008, pp. C661–C676

[17] J. D. Berry, M. R. Davidson, D. J. E. Harvie, An electrokinetic flow model of electrolytes with liquid/liquid inferfaces, *in preparation for Journal of Computational Physics*, 2012